Above-threshold detachment of negative ions by circularly polarized few-cycle laser fields

Lihua Bai (白丽华)*, Yuheng Liu (刘宇恒), Tingting Cui (崔婷婷), Yan Wang (王 燕), Dongmei Deng (邓冬梅), and Huifang Zhang (张惠芳)

Department of Physics, Shanghai University, Shanghai 200444, China

**Corresponding author: lhbai@163.com*

Received August 2, 2010; accepted September 21, 2010; posted online January 1, 2011

In accordance with nonperturbative quantum scattering theory, we investigate photoelectron angular distributions (PADs) from above-threshold detachment (ATD) of negative ions irradiated by circularly polarized few-cycle laser fields. Electrons ejected on the polarization plane demonstrate distinct anisotropies in angular distributions which distinctly vary with the carrier-envelope (CE) phase. The anisotropy is caused by interference between transition channels; it also depends strongly on laser frequency, pulse duration, and kinetic energy of photoelectrons. Optimal emission of photoelectrons, which varies with CE phase, makes it possible to control photoelectron motion.

OCIS codes: 020.4180, 020.2649.

doi: 10.3788/COL201109.010202.

With the rapid development in laser technology, it has become possible to produce ultrashort laser pulses containing only a few optical cycles[1,2]. The temporal shape of electric fields dramatically varies with the initial phase of carrier waves with respect to pulse envelopes (also referred to as carrier-envelope (CE) phase). The CE phase plays an important role in the interaction of matters with short pulses[3,4]. In recent research, the study of detachment of negative ions has aroused both theoretical and experimental interests[5−17], and the above-threshold detachment (ATD) in few-cycle limit and CE phase-dependent phenomena have become prominent subject fields as well[18,19]. Given the lack of Coulomb attraction of detached electrons by parent ions, as well as the loosely bound and easily detached outermost electron of negative ions, the negative ion detachment in the strong field could provide perfect investigation of strong-field approximation[20].

In a recent theoretical study, Bivona *et al*. have investigated the photodetachment of F^- irradiated by a few-cycle circularly polarized laser field through a two-step semi-classical model[18]. They have discussed the effects of CE phase and the number of cycles contained in a pulse (also referred to as cycle number) on the potoelectron angular distributions (PADs), and found that the anisotropies in PADs of electrons ejected on the plane perpendicular to the laser propagation direction were dependent on the cycle number of laser pulse. They have also established that the anisotropy in PADs is strongly reduced with increase in cycle number.

By using a nonperturbative quantum scattering theory, we investigate the PADs of ATD for negative ion H^- irradiated by circularly polarized few-cycle laser fields. PADs vary with CE phase. Electrons ejected on the plane perpendicular to the laser propagation contain distinct anisotropies in angular distributions, which strongly depend on cycle number, kinetic energy of the photoelectron, and laser frequency. We have demonstrated that the anisotropies in PADs are more distinct when the cycle number is smaller, the kinetic energy is higher, and the laser frequency is lower. These findings offer possible means of controlling PADs during anisotropic photoionization.

Short pulse can comprise three quantized laser modes[21],

$$\omega_1 = \omega, \quad \omega_2 = \omega(1 + 1/n), \quad \omega_3 = \omega(1 - 1/n),$$

where n denotes the cycle number.

Under such modulation, the synthesized electric field behaves as an infinite sequence of identical, few-cycle laser pulses, which can be described as

$$\begin{aligned} E(t) &= E_0[2\sin(\omega_1 t + \phi_0) - \sin(\omega_2 t + \phi_0) \\ &\quad - \sin(\omega_3 t + \phi_0)]/4 \\ &= E_0 \sin^2(\omega t/2n)\sin(\omega t + \phi_0), \end{aligned} \tag{1}$$

where E_0 is the peak value of the synthesized electric field and ϕ_0 is the CE phase. The first term can be regarded as the envelope of an infinite sequence of n-cycle pulses, whereas the second term acts as the carrier wave. Thus, the synthesized field corresponds to a series of n-cycle pulses, each sharing a common phase (ϕ_0). In this letter, the peak intensity of the synthesized n-cycle pulses is referred to as laser intensity.

The transition rate for a given ATD peak in the pulse sequences is given by ($\hbar = 1, c = 1$)[21]

$$\begin{aligned} \frac{\mathrm{d}^2 W}{\mathrm{d}\Omega_{\mathrm{P}_f}} =& \frac{(2m_{\mathrm{e}}^3\omega^5)^{1/2}}{(2\pi)^2}(q - \varepsilon_{\mathrm{b}})^{1/2}(q - 4u_{p1})^2 \mid \Phi_i(\mathbf{P}_{\mathrm{f}} - q\mathbf{k}) \mid^2 \\ &\times \mid \sum_{q_i, j_i} \aleph_{-j_1,-j_2,-j_3}(z_f)^* \aleph_{q_1-j_1,q_2-j_2,q_3-j_3}(z_{\mathrm{f}}) \mid^2, \end{aligned} \tag{2}$$

where m_{e} is the rest mass of the electron while q is the absorbed-photon number with

$$q\omega = q_1\omega_1 + q_2\omega_2 + q_3\omega_3, \tag{3}$$

with q_i (i=1,2,3) as the overall transferred photon number of the ith mode. The sum over q_i is performed over

all possible q_1, q_2, q_3 for a fixed q. We identified one set of q_i satisfying Eq. (3) for a fixed q and used this as transition channel. Channels that are indistinguishable with $q_2 = q_3$ are regarded as one. In the equation, integer q corresponds to the final kinetic energy of the photoelectrons:

$$E_k \equiv \frac{\mathbf{P}_f^2}{2m_\mathrm{e}} = q\omega - E_\mathrm{b}. \tag{4}$$

Ponderomotive parameters $u_p, u_{p1}, u_{p2}, u_{p3}$ are given by $u_p = \frac{e^2\Lambda^2}{m_\mathrm{e}\omega}, u_{pi} = \frac{e^2\Lambda_i^2}{m_\mathrm{e}\omega_i}, (i = 1, 2, 3)$, with 2Λ being the classical amplitude of the laser field and $2\Lambda_i$ being the classical amplitude of ith classical field; E_b is the ionic binding energy. In Eq. (2), $\varepsilon_\mathrm{b} = E_\mathrm{b}/(\hbar\omega)$ is the binding number, i.e., the ionic binding energy E_b in units of laser photon energy $\hbar\omega$; $\mathbf{P}_f$ is the final momentum of the photoelectron, $\mathbf{k}$ is the central wave vector of the laser pulse, and $\Phi_i(\mathbf{P}_f)$ is the angular eigenstate of the negative ion. The quantity, $j_i (i = 1, 2, 3)$, is the number of photons absorbed in the detachment process in the ith mode and is a mute number in the sum. We performed a summation of $j_i (i = 1, 2, 3)$ on the energy shell. The three-mode generalized phased Bessel (GPB) functions are given by[21]

$$\begin{aligned}\aleph_{-j_1,-j_2,-j_3}(z_f) = &\\ \sum_{m_5,m_7,m_9} & X_{j_1-m_5-m_7}(\zeta_{1f}) X_{j_2+m_5-m_9}(\zeta_{2f})\\ \times & X_{j_3+m_7+m_9}(\zeta_{3f}) X_{m_5}(z_5) X_{m_7}(z_7) X_{m_9}(z_9),\end{aligned} \tag{5}$$

The sum is calculated for integer indices

$$m_i (i = 1, \cdots, 9) : -\infty < m_i < +\infty.$$

Meanwhile, $X_n(z)$ is the phased Bessel function.

The arguments of the GPB function are[21]

$$\begin{aligned}\zeta_{1f} &= \frac{2|e|\Lambda_1}{m_\mathrm{e}\omega_1}\mathbf{P}_f \cdot \boldsymbol{\varepsilon}_1, \quad \zeta_{2f} = \frac{2|e|\Lambda_2}{m_\mathrm{e}\omega_2}\mathbf{P}_f \cdot \boldsymbol{\varepsilon}_2,\\ \zeta_{3f} &= \frac{2|e|\Lambda_3}{m_\mathrm{e}\omega_3}\mathbf{P}_f \cdot \boldsymbol{\varepsilon}_3, \quad z_5 = \frac{2e^2\Lambda_1\Lambda_2\boldsymbol{\varepsilon}_2 \cdot \boldsymbol{\varepsilon}_1^*}{m_\mathrm{e}(\omega_2 - \omega_1)},\\ z_7 &= \frac{2e^2\Lambda_1\Lambda_3\boldsymbol{\varepsilon}_3 \cdot \boldsymbol{\varepsilon}_1^*}{m_\mathrm{e}(\omega_3 - \omega_1)}, \quad z_9 = \frac{2e^2\Lambda_2\Lambda_3\boldsymbol{\varepsilon}_2 \cdot \boldsymbol{\varepsilon}_3^*}{m_\mathrm{e}(\omega_3 - \omega_2)}.\end{aligned} \tag{6}$$

where $\boldsymbol{\varepsilon}_i (i = 1, 2, 3)$ is the polarization vector of the ith mode defined as

$$\begin{aligned}\boldsymbol{\varepsilon}_i &= [\boldsymbol{\varepsilon}_x \cos(\xi/2) + \mathrm{i}\boldsymbol{\varepsilon}_y \sin(\xi/2)]\mathrm{e}^{\mathrm{i}\varphi_i},\\ \boldsymbol{\varepsilon}_\mathrm{i}^* &= [\boldsymbol{\varepsilon}_x \cos(\xi/2) - \mathrm{i}\boldsymbol{\varepsilon}_y \sin(\xi/2)]\mathrm{e}^{-\mathrm{i}\varphi_i},\\ \boldsymbol{\varepsilon}_\mathrm{i} \cdot \boldsymbol{\varepsilon}_k &= \cos(\xi)\mathrm{e}^{\mathrm{i}(\phi_\mathrm{i}+\phi_k)}, \boldsymbol{\varepsilon}_i \cdot \boldsymbol{\varepsilon}_k^* = \mathrm{e}^{\mathrm{i}(\phi_i-\phi_k)},\end{aligned} \tag{7}$$

where $\boldsymbol{\varepsilon}_x$ and $\boldsymbol{\varepsilon}_y$ are the unit vectors vertical to each other, ξ monitors the polarization degree (i.e., $\xi = 0$ denotes linear polarization, $\xi = \pi/2$ represents circular polarization). Phase angle $\phi_i (i = 1, 2, 3)$ relates to CE phase ϕ_0 as

$$\phi_1 = \pi, \quad \phi_2 = -\phi_0/n, \quad \phi_3 = \phi_0/n. \tag{8}$$

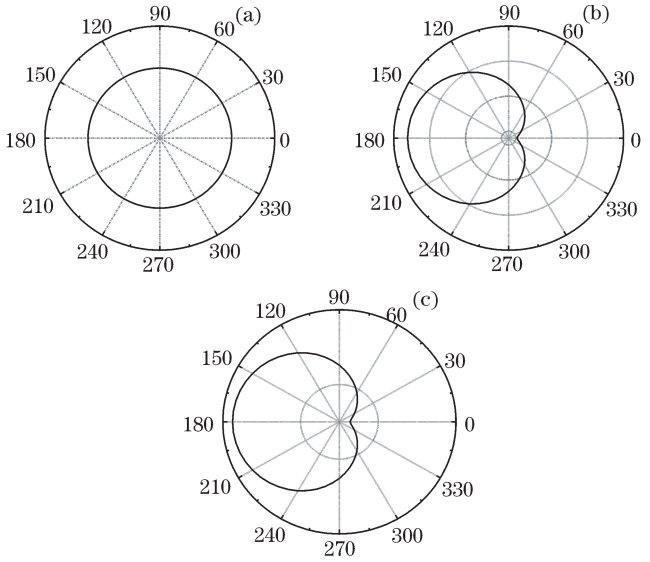

Fig. 1. Polar plots of the calculated PADs of the third ATD peaks for negative ion H^- in circularly polarized (a) five cycle, (b) four cycle, and (c) three cycle laser pulses with CE phase at 0°. The laser intensity is 0.4 TW/cm^2 and the laser wavelength 1800 nm.

Accordingly, $\mathrm{d}\Omega_{P_f} = \sin\theta_f \mathrm{d}\theta_f \mathrm{d}\phi_f$ is the differential solid angle of the final photoelectron, where θ_f and ϕ_f are the scattering and azimuthal angles, respectively. PAD denotes the detachment rate for different ϕ_f at fixed $\theta_f = \pi/2$.

In this letter, we identified negative ion H^- as the sample ion. In our calculations, the binding energies were 0.75421 eV for negative ion H^-[22]. The initial wave function was chosen as the ground-state wave function. Our calculations showed distinct anisotropies in PADs of electrons were ejected on the plane perpendicular to the laser propagation from the ATD of negative ions by few-cycle laser pulses. The anisotropy in PADs depended strongly on laser frequency, kinetic energy of the photoelectron, and cycle number. The PADs were strongly influenced by CE phase. The anisotropy was caused by the numerous channel transitions. Correspondingly, the interference among different transition channels induced the anisotropy, and most of the emitted direction of photoelectrons was determined by the CE phase[21].

We investigated the influence of cycle number on PADs for negative ion H^- by inducing few-cycle circularly polarized laser pulses (Fig. 1). In the calculations, the laser intensity was 0.4 TW/cm^2 while the laser wavelength was 1800 nm. Based on Fig. 1, the PADs are not always isotropic; with a decrease in cycle number, anisotropy in PADs appears. Figure 1(a) on the five-cycle laser pulses shows that the PAD is isotropic. As cycle number decreased, the PADs became anisotropic. This is prominent in Fig. 1(b) for cycle number n=4 and Fig. 1(c) for cycle number n=3; these findings are in agreement with that proposed by Bivona *et al.*[18]. The maximum number of emitted photoelectrons was located at ϕ_f=180° while the minimum was located at ϕ_f=0°. For cycle number n=5, only one transition channel was observed; there was also no interference and the PAD was isotropic. For cycle numbers n=4 and n=3, there were three and two transition channels, respectively, and

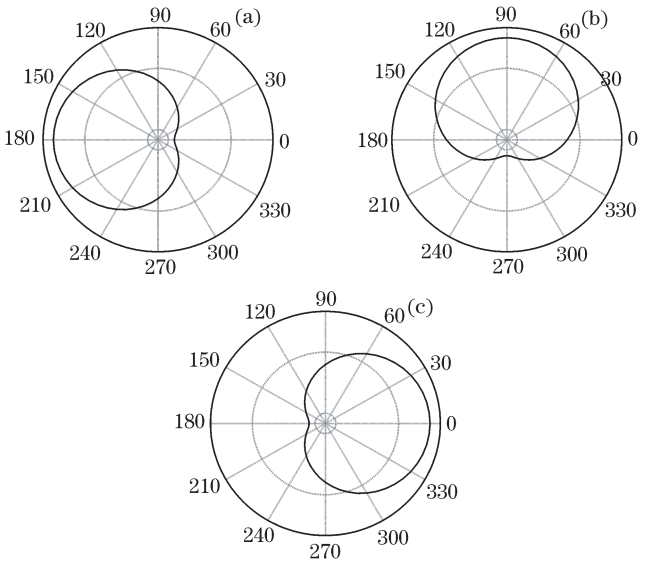

Fig. 2. Polar plots of the calculated PADs of the third ATD peaks for negative ion H^- in three-cycle circularly polarized laser pulses at different CE phases. (a) 0°, (b) 90°, and (c) 180°. Laser intensity is 0.5 TW/cm^2 and laser wavelength is 2400 nm.

the interference between different transition channels induced the anisotropies in PADs.

We further investigated the influence of CE phase, kinetic energy of the photoelectron, and laser frequency on PADs. Figure 2 shows the calculated PADs of the third ATD peak for several CE phases for laser pulses with intensity of 0.5 TW/cm^2 and wavelength of 2400 nm. Figures 2(a)–(c) correspond to different CE phases of ϕ_0=0°, 90°, and 180°, respectively. As shown in Fig. 2, PADs vary with CE phase. For $\phi_0 = 0°$ and ϕ_0=180°, the number of photoelectrons emitted to the right is not the same as that to the left, as shown in Figs. 2(a) and (c). For ϕ_0 =90°, as shown in Fig. 2(b), the number of photoelectrons emitted to the right is the same as that to the left.

The position of the maximum also varied with CE phase because of the corresponding direction of the maximal electric-field strength. For ϕ_0=0°, the maximum was located at ϕ_f=180° while the minimum was located at ϕ_f=0°. For ϕ_0=180°, the maximum was located at the right and the minimum was located at the left. For ϕ_0=90°, although the number of photoelectrons emitted to the right was the same as that to the left, the maximum of PADs was located at ϕ_f=90°, and the minimum at ϕ_f=270°.

The maximal ionization rate was constant across the various CE phases. This phenomenon indicates that the maximal field strength of the synthesized circularly polarized pulses remains constant as well. Owing to the symmetry of electric field with respect to its maximum, the photoelectrons emitted to the left and right directions were symmetric near the axis (i.e., depending on the CE phase). For the few-cycle circularly polarized laser pulses, the electric field of pulses varied with CE phase. Notably, the CE phase would determine the direction of the maximal field, and the intense-matter interaction was dependent on the electric field of the pulse. Accordingly, the CE phase influenced the maximal occupation

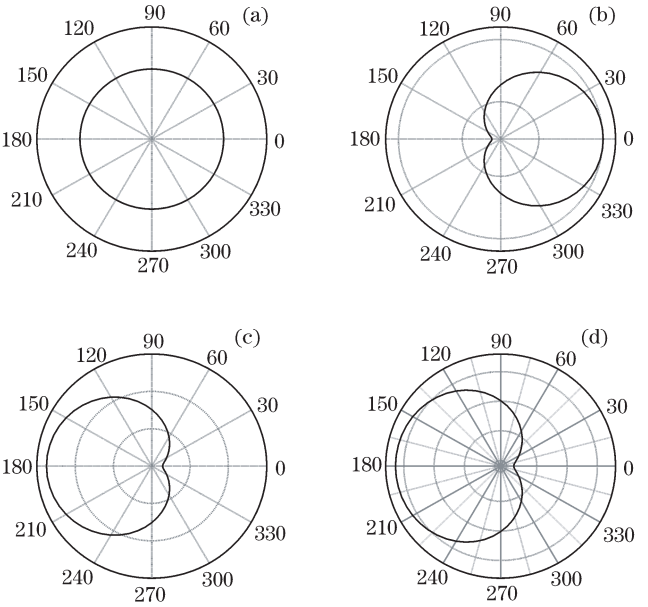

Fig. 3. Polar plots of the calculated PADs of the (a) first, (b) second, (c) third, and (d) fourth ATD peaks for negative ion H^- in three-cycle circularly polarized laser pulses. (a)–(d): Photoelectron energies of 0.69, 1.38, 2.07, and 2.76 eV, respectively. Laser intensity is 0.4 TW/cm^2, laser wavelength is 1800 nm, and CE phase is 0°.

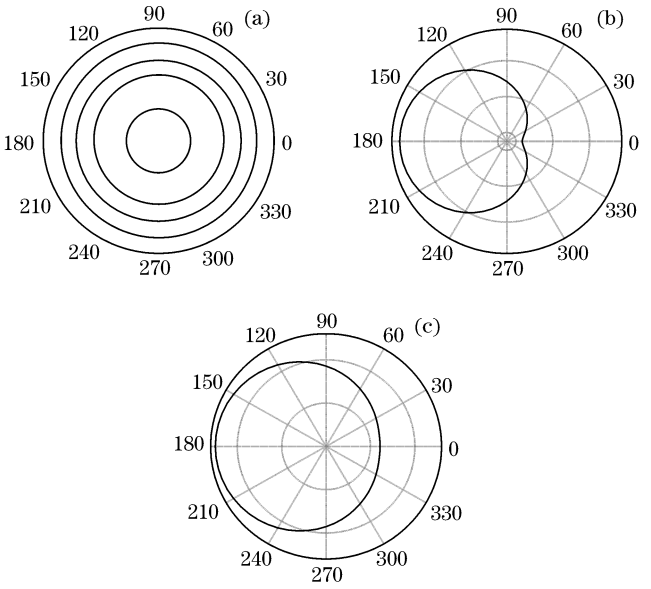

Fig. 4. Polar plots of calculated PADs of the first ATD peak for negative ion H^- in three-cycle circularly polarized laser pulses at different laser wavelengths. (a) 1800, (b) 3400, and (c) 3600 nm. Peak laser intensity is 0.4 TW/cm^2 and CE phase is 0°.

direction of the photoelectrons. These results were consistent with the analysis of Paulus *et al.*[3].

Figure 3 shows the influence of the kinetic energy of the photoelectron on the PADs of negative ion H^- in three-cycle circularly polarized laser fields. In the calculation, the laser intensity was 0.4 TW/cm^2, the laser wavelength was 1800 nm, and the CE phase was 0°. The PADs were anisotropic for higher kinetic energy. As for the first ATD peak in Fig. 3(a) with photoelectron energy of 0.69

eV, the PADs are isotropic. For higher kinetic energies, the PADs become anisotropic, as shown in Figs. 3(b)–(d); these figure insets correspond to the second, third, and fourth ATD peaks, with photoelectron energies of 1.38, 2.07, and 2.76 eV, respectively. For the higher kinetic energy of photoelectrons, many transition channels were observed. The quantum interference of the different transitions caused the PADs to become anisotropic. For the lower kinetic energy of photoelectrons, only one transition channel was demonstrated; thus, the PADs were isotropic.

Figure 4 shows the influence of laser frequency on the PADs. In the calculation, the laser intensity was 0.4 TW/cm^2 and the CE phase was 0°. Based on Fig. 4, the PADs are anisotropic for longer laser wavelengths. In Fig. 4(a), which presents the laser wavelength of 1800 nm, the PADs are isotropic. For longer laser wavelengths, the PADs are anisotropic, as shown in Figs. 4(b) and (c). Accordingly, many transition channels could be observed. The quantum interference of different transitions caused anisotropy in the PADs. In contrast, for shorter laser wavelengths, only one transition channel existed, resulting in isotropy in PADs.

In conclusion, we show that PADs in circularly polarized few-cycle laser pulses are anisotropic and vary distinctly with CE phase. The ionization rates in opposite directions are not always equal to each other. Accordingly, the anisotropy is caused by the interference between transition channels; it depends strongly on laser frequency, pulse duration, and kinetic energy of photoelectrons. Given that the optimal emission of photoelectrons varies with CE phase, control of the photoelectron motion can achieved.

This work was supported by the National Natural Science Foundation of China under Grant Nos. 60908006, 10804067, and 60407007.

References

1. M. Nisoli, S. De Silvestri, O. Svelto, R. Szipöcs, K. Ferencz, C. Spielmann, S. Sartania, and F. Krausz, Opt. Lett. **22,** 522 (1997).
2. B. C. Stuart, M. D. Perry, J. Miller, G. Tietbohl, S. Herman, J. A. Britten, C. Brown, D. Pennington, V. Yanovsky, and K. Wharton, Opt. Lett. **22,** 242 (1997).
3. G. G. Paulus, F. Grasbon, H. Walther, P. Villoresi, M. Nisoli, S. Stagira, E. Priori, and S. De Silvestri, Nature **414,** 182 (2001).
4. G. G. Paulus, F. Lindner, H. Walther, A. Baltuška, E. Goulielmakis, M. Lezius, and F. Krausz, Phys. Rev. Lett. **91,** 253004 (2003).
5. R. Reichle, H. Helm, and I. Y. Kiyan, Phys. Rev. A. **68,** 063404 (2003).
6. Y. Huang and S. Liu, Chinese J. Lasers (in Chinese) **36,** 3133 (2009).
7. D. A. Telnov and S. I. Chu, Phys. Rev. A. **66,** 063409 (2002).
8. D. A. Telnov and S. I. Chu, J. Phys. B: At. Mol. Opt. Phys. **29,** 4401 (1996).
9. X. Fang, Q. Wang, J. Liu, B. Liu, Y. Li, L. Chai, and M. Hu, Chinese J. Lasers (in Chinese) **37,** 1585 (2010).
10. J. Wang, S. I. Chu, and C. Laughlin, Phys. Rev. A. **50,** 3208 (1994).
11. D. A. Telnov and S. I. Chu, Phys. Rev. A. **59,** 2864 (1999).
12. D. A. Telnov and S. I. Chu, Phys. Rev. A. **66,** 043417 (2002).
13. W. W. Smith, C. Y. Tang, C. R. Quick, H. C. Bryant, P. G. Harris, A. H. Mohagheghi, J. B. Donahue, R. A. Reeder, H. Sharifian, J. E. Stewart, H. Toutounchi, S. Cohen, T. C. Altman, and D. C. Risolve, J. Opt. Soc. Am. B. **8,** 17 (1991).
14. C. Y. Tang, H. C. Bryant, P. G. Harris, A. H. Mohagheghi, R. A. Reeder, H. Sharifian, H. Tootoonchi, C. Quick, J. Donahue, S. Cohen, and W. Smith, Phys. Rev. Lett. **66,** 3124 (1991).
15. C. Y. Tang, P. G. Harris, A. H. Mohagheghi, H. C. Bryant, C. R. Quick, J. B. Donahue, R. A. Reeder, S. Cohen, W. W. Smith, and J. E. Stewart, Phys. Rev. A. **39,** 6068 (1989).
16. G. Haeffler, D. Hanstorp, I. Kiyan, A. E. Klinkmuller, U. Ljungblad, and D. J. Pegg, Phys. Rev. A. **53,** 4127 (1996).
17. I. Y. Kiyan and H. Helm, Phys. Rev. Lett. **90,** 183001 (2003).
18. S. Bivona, R. Burlon, and C. Leone, Opt. Express **14,** 12576 (2006).
19. S. Bivona, R. Burlon, G. Ferante, and C. Leone, Opt. Express **14,** 3715 (2006).
20. R. Reichle, H. Helm, and I. Y. Kiyan, Phys. Rev. Lett. **87,** 243001 (2001).
21. J. Zhang and Z. Xu, Phys. Rev. A. **68,** 013402(2003).
22. T. Andersen, H. K. Haugen, and H. Hotop, J. Phys. Chem. Ref. Data **28,** 1511 (1999).